<u>Electronic Supplementary Information</u>

Vibrational frequencies utilized for the assessment of exchange-correlation functionals in the description of metal-adsorbate systems: C_2H_2 and C_2H_4 on transition-metal surfaces

Ray Miyazaki,[*,†,‡,§] Somayeh Faraji,[†,§] Sergey V. Levchenko,[¶] Lucas Foppa,[*,†] and

Matthias Scheffler[†]

†The NOMAD Laboratory at the Fritz-Haber-Institute of the Max-Planck-Gesellschaft and IRIS-Adlershof of the Humboldt-Universität zu Berlin, Faradayweg 4-6, D-14195 Berlin, Germany

‡Institute for Catalysis, Hokkaido University, N21 W10 Kita-ku, Sapporo, Hokkaido, 001-0021, Japan

¶Center for Energy Science and Technology, Skolkovo Institute of Science and Technology, Moscow 121205, Russia

§These authors contributed equally

E-mail: ray_miyazaki@cat.hokudai.ac.jp; foppa@fhi-berlin.mpg.de

S1. Geometry analysis of C_2H_2 and C_2H_4

Geometry optimizations for the molecules in the gas phase are performed. The obtained geometrical parameters are listed in Table S1 along with the corresponding experimental values.

Table S1: Calculated and experimental geometrical parameters (bond lengths d and angles ∠ in Å and degree, respectively) for the C_2H_2 and C_2H_4 molecules in the gas phase.

C_2H_2	mBEEF	RPBE	Exp.[1]
d_{CH} (Å)	1.059	1.070	1.061
d_{CC} (Å)	1.194	1.210	1.203
C_2H_4	mBEEF	RPBE	Exp.[2]
d_{CC} (Å)	1.322	1.337	1.337±0.003
d_{CH} (Å)	1.081	1.092	1.086±0.003
∠ (HCC)	121.78	121.75	121.35±1
∠ (HCH)	116.4	116.5	
∠ ((CH$_2$)-C)	179.97	179.94	180.00

S2. Bulk lattice constants

Table S2: Bulk lattice constant a (in Å) of each material in its stable crystal phase (FCC structure with space group $Fm\bar{3}m$) obtained by mBEEF and RPBE XC functionals. A k-point mesh of 20×20×20 was used for each calculation. The values in parentheses next to the mBEEF and RPBE values indicate the deviation from experimental results. Last row shows the mean absolute percentage error (MAPE) of each functional. mBEEF(QHA) and RPBE(QHA) are the results incorporating thermal effects via the quasi-harmonic approximation (QHA) at the experimental temperature at which the lattice constants were measured. The QHA was evaluated using the phonon analysis as implemented in Phonopy.[28]

compound	mBEEF	mBEEF (QHA)	RPBE	RPBE (QHA)	Exp.
Pd	3.887 (-0.004)	3.904 (0.013)	3.977 (0.086)	3.993 (0.102)	3.891 (295.15 K)[3]
Pt	3.916 (-0.008)	3.902 (-0.022)	3.939 (0.015)	4.006 (0.082)	3.924 (298.15 K)[27]
Rh	3.769 (-0.035)	3.781 (-0.023)	3.851 (0.047)	3.862 (0.058)	3.804 (294.65 K)[3]
Cu	3.575 (-0.040)	3.588 (-0.027)	3.674 (0.059)	3.691 (0.076)	3.615 (291.15 K)[3]
MAPE (in %)	0.589	0.562	1.342	2.085	-

S3. Vibrational modes

Figure S1 illustrates different vibrational modes of acetylene and ethylene in gas phase. Arrows in orange are showing the movement direction. Dot and cross marks inside the orange circles are used to show the movement direction. Here, we briefly describe the movements of atoms in each type of the vibrational modes. As shown in the figure, "twisting" modes are related to a change in the angle between planes containing groups of atoms. "Rocking" modes represent a change in the angle between the group of H-C-H atoms (shown in pink) and the rest of the molecule. A change in the angle between the plane of a group of H-C-H atoms (shown in pink) and a plane through the rest of the molecule refers to "wagging" modes. Rocking is distinguished from wagging by the fact that the atoms in the group stay in the same plane as the rest of the ethylene molecule. The in-plane and out-of-plane bending modes are denoted by δ and γ, respectively. In a rocking, wagging or twisting coordinate the bond lengths within the atomic groups involved slightly change. So the dominant movements are in the angles.
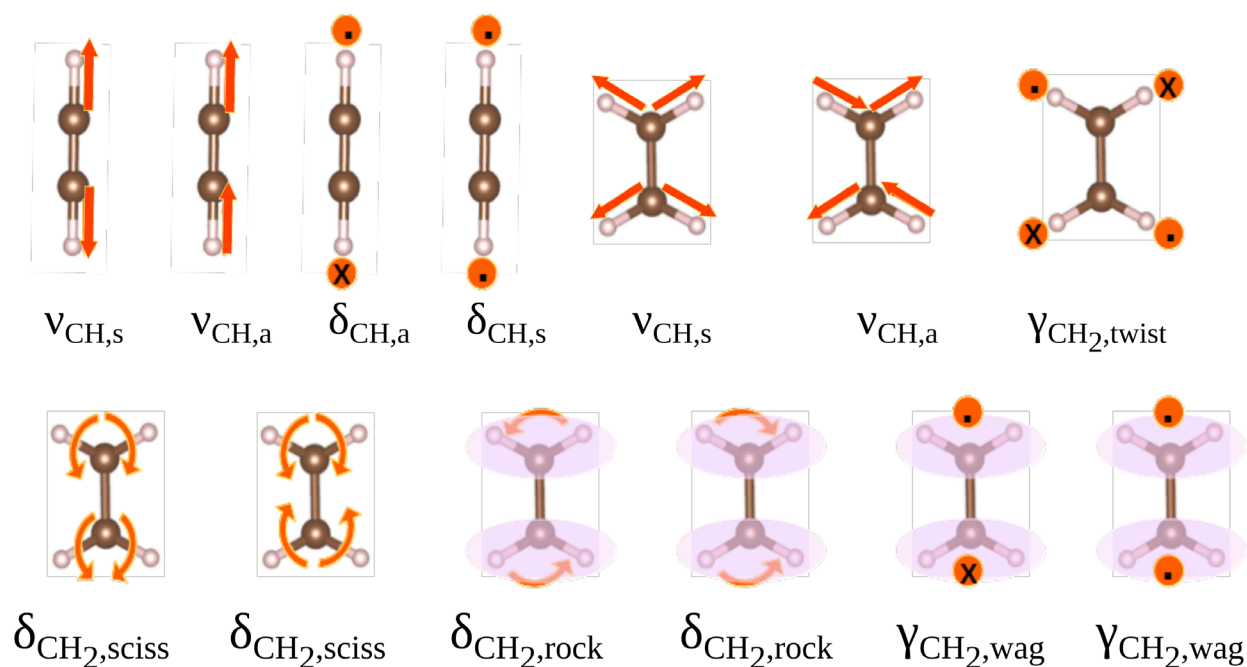
Figure S1: Vibrational modes of acetylene and ethylene in gas phase. ν, δ and γ denote stretch mode, in-plane bending mode and out-of-plane bending mode, respectively. "a" and "s" represent asymmetric and symmetric stretches, respectively. Dot and cross marks inside the orange circles denote the out-of-plane movement direction of an atom or group of atoms.

S4. Vibrational frequencies of C_2H_2 and C_2H_4 in the gas phase

The calculated vibrational frequencies of C_2H_2 and C_2H_4 in the gas phase and the corresponding experimental values are summarized in Table S3 (detailed description of each vibrational mode is provided in the previous section and shown in FIG. S1). C_2H_2 is a symmetric linear molecule with $3N - 5 = 7$ normal modes. However, only five modes are reported in the table because the bending modes come in degenerate pairs, i.e., there are two equivalent modes with the same frequency. According to the calculated data shown in the table, the vibrational frequencies obtained by the mBEEF functional are overestimated while the RPBE functional underestimates them: the mean percentage error ($\mathrm{MPE} = \frac{100}{16} \sum_{i=1}^{16} \frac{\mathrm{DFA_i} - \mathrm{Exp_i}}{\mathrm{Exp_i}}$) of all the considered vibrational modes summarized in Table S3 obtained by mBEEF and RPBE are 3.04% and −0.13%, respectively.

To simplify the comparison, the frequency differences of each vibrational mode of the C_2H_2 and C_2H_4 molecules (in gas phase) with respect to the experimental values are shown in the FIG. S2. Our analysis shows that the root mean square error (RMSE) of the vibrational frequencies obtained with RPBE is smaller than for mBEEF by 79 cm^{-1} for C_2H_2 and 58 cm^{-1} for C_2H_4.

Another notable result in the FIG. S2 is the larger deviation of the mBEEF results for the stretching modes while the bending modes (rocking, wagging, and scissoring) display smaller deviations. From comparison of calculated vibrational frequencies of stretching modes with experiment it can be inferred that mBEEF overestimates the strength of the bonds. However, the electrostatic interactions and orbital hybridization determining the bending force constants are less affected by the approximations in the XC functional, which results in smaller frequency deviations for bending-type vibrational modes.
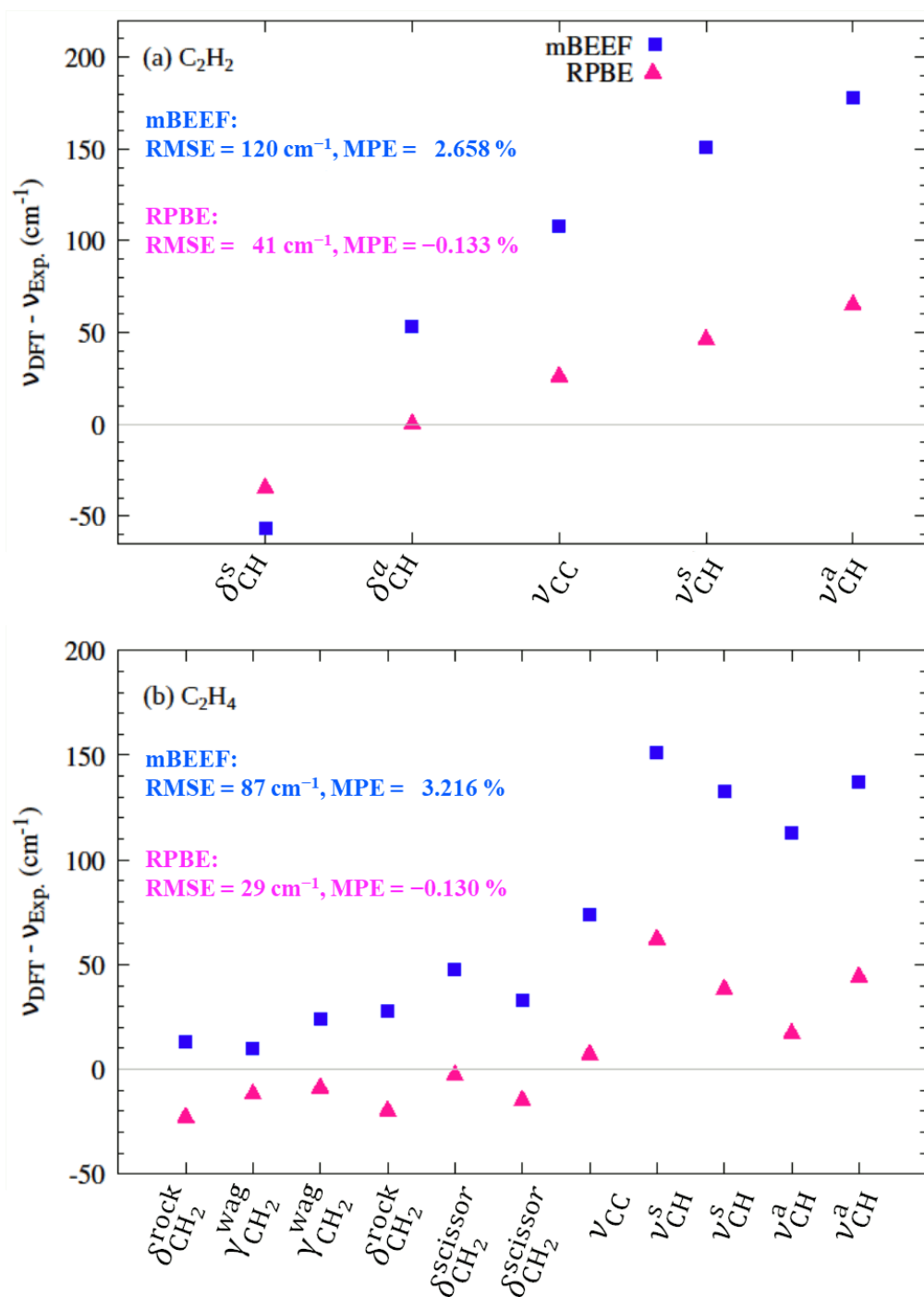
Figure S2: Deviations of calculated vibrational frequencies of C_2H_2 and C_2H_4 molecules in gas phase from experimental values. The blue squares and pink triangles indicate the deviations for mBEEF and RPBE functionals, respectively. (See Table S3 for the values of vibrational frequencies and experimental references.) RMSE and MPE denote root mean squared error and mean percentage error, respectively.

Table S3: The vibrational frequencies (in cm^{-1}) of the C_2H_2 and C_2H_4 molecules in the gas phase. ν, δ and γ denote stretch mode, in-plane bending mode and out-of-plane bending mode, respectively. "a" and "s" denote asymmetric and symmetric modes, respectively. RMSE and MPE denote the values of root mean squared error and mean percentage error, respectively.

C_2H_2	mBEEF	RPBE	Exp.[4]
δ^s_{CH}	555	578	612
δ^a_{CH}	782	730	729
ν_{CC}	2082	2001	1974
ν^s_{CH}	3446	3342	3295
ν^a_{CH}	3551	3439	3373
RMSE (cm^{-1})	120	41	
MPE (%)	2.658	-0.133	
C_2H_4	mBEEF	RPBE	Exp.[5]
δ^{rock}_{CH2}	839	804	826
γ^{wag}_{CH2}	950	929	940
γ^{wag}_{CH2}	973	941	949
$\gamma^{twist,}_{CH2}$	1080	1032	-
δ^{rock}_{CH2}	1250	1203	1222
$\delta^{scissor}_{CH2}$	1390	1340	1342
$\delta^{scissor}_{CH2}$	1477	1430	1444
ν_{CC}	1697	1631	1623
ν^s_{CH}	3140	3052	2989
ν^s_{CH}	3159	3065	3026
ν^a_{CH}	3216	3121	3103
ν^a_{CH}	3242	3150	3105
RMSE (cm^{-1})	87	29	
MPE (%)	3.216	-0.130	

S5. Vibrational frequencies of adsorbed C_2H_2 and C_2H_4

Table S4 summarizes the chamber exposures and the reported coverage for the adsorbed species.

The vibrational frequencies of adsorbed C_2H_2 and C_2H_4 on FCC(111) surfaces of Pt, Pd, Rh, and Cu are summarized in Table S5.

Table S4: Experimental/theoretical data on the coverage (θ in ML) and gas exposure (P in L, 1L= 1 langmuir = 1×10⁻⁶ Torr-second) for the adsorbed systems.

system	P	θ
C_2H_2/Pd(111)[6]	3	1/3
C_2H_2/Pd(111)[7]	1.5	1/3
C_2H_2/Rh(111)[8]	0.5	1/4
C_2H_2/Cu(111)[9]	2.3	
C_2H_2/Pt(111)[10]	2	
C_2H_4/Cu(111)[11]	100	1/3
C_2H_4/Pd(111)[12]	30	

Table S5: Calculated and experimental vibrational frequencies (in cm⁻¹) for C_2H_2 and C_2H_4 adsorbed on different TMSs at the coverage of 1/9 ML and 1/4 ML. The values for 1/4 ML are shown in parentheses. Stretch modes are labeled by ν, while δ and γ denote in-plane and out-of-plane bending modes, respectively.

mode	method	Pt(111)	Pd(111)	Rh(111)	Cu(111)
C_2H_2		(fcc-par)	(fcc-par)	(fcc-par)	(b-per)
$\nu_{CH,s}$	Exp.	3010[10]	2990,[6] 2992[7]	2960[8]	2920,[9]2913[13]
	mBEEF	3164(3146)	3145(3132)	3121(3190)	3090(3069)
	RPBE	3078(3065)	3064(3057)	3043(3036)	3003(2992)
ν_{CC}	Exp.	1310[10]	1400,[6]1402[7]	1260[8]	1307,[9]1294[13]
	mBEEF	1324(1335)	1353(1365)	1295(1298)	1325(1352)
	RPBE	1262(1273)	1303(1316)	1238(1241)	1261(1291)
$\delta_{CH,a}$	Exp.	985[10]	1034 [7]	1120[8]	920,[9]920[13]
	mBEEF	1170(1170)	1090(1087)	1132(1127)	1152(1144)
	RPBE	1119(1119)	1033(1030)	1078(1073)	1105(1100)
$\delta_{CH,s}$	Exp.	—	872 [7]	950[8]	—
	mBEEF	1017(1024)	929(946)	967(985)	964(973)
	RPBE	976 (985)	885(900)	924(941)	925(935)
$\gamma_{CH,a}$	Exp.	—	880 [6]	—	—

Continued on next page

Table S5 – *Continued from previous page*

		Pt(111)	Pd(111)		
C$_2$H$_4$		(b-par)	(b-par)		
	mBEEF	872(869)	795(792)	833(825)	914(915)
	RPBE	837(831)	766(761)	802(793)	882(887)
$\gamma_{\mathrm{CH,s}}$	Exp.	770[10]	660,[6]673[7]	720[8]	680[9]
	mBEEF	796(794)	710(706)	733(726)	690(671)
	RPBE	759(752)	678(672)	704(695)	659(644)
$\nu_{\mathrm{MC,s}}$	Exp.	570[10]	500 [7]	—	420[9]
	mBEEF	579(593)	532(539)	562(558)	428(435)
	RPBE	546(557)	482(489)	515(513)	394(401)
$\nu^{\mathrm{a}}_{\mathrm{CH2}}$	Exp.	3000 [14]	—		
	mBEEF	3133(3111)	3129(3112)		
	RPBE	3051(3041)	3060(3052)		
$\nu^{\mathrm{s}}_{\mathrm{CH}}$	Exp.	2940 [10]	2900,[12]2928[11]		
	mBEEF	3077(3062)	3066(3055)		
	RPBE	2992(2989)	2993(2989)		
$\nu^{\mathrm{s}}_{\mathrm{CH2}}$	Exp.	2920 [14]	–		
	mBEEF	3065(3048)	3054(3040)		
	RPBE	2985(2977)	2985(2978)		
$\delta^{\mathrm{scissor,s}}_{\mathrm{CH2}}$	Exp.	1430 [14]	1428 [11]		
	mBEEF	1470(1471)	1478(1478)		
	RPBE	1422(1423)	1433(1433)		
ν_{CC}	Exp.	1050 [14]	1103,[12]1097[11]		
	mBEEF	1023(1022)	1102(1095)		
	RPBE	980(983)	1087(1081)		

		Pt(111)	Pd(111)	
C_2H_4		(b-par)	(b-par)	
$\gamma_{CH2}^{wag,s}$	Exp.	980[14]	871 [11]	
	mBEEF	976(980)	910(913)	
	RPBE	932(937)	862(869)	
$\gamma_{CH2}^{twist,s}$	Exp.	790[14]	—	
	mBEEF	819(811)	796(782)	
	RPBE	790(781)	786(770)	
$\delta_{CH2}^{rock,s}$	Exp.	660[14]	—	
	mBEEF	683(678)	603(594)	
	RPBE	649(644)	552(545)	
ν_{MC}^{a}	Exp.	560[14]	—	
	mBEEF	587(591)	512(515)	
	RPBE	546(549)	447(453)	
ν_{MC}^{s}	Exp.	470[10,14]	—	
	mBEEF	493(499)	437(443)	
	RPBE	450(454)	359(370)	

[6] T=130 K, 3L C_2H_2,$(\sqrt{3} \times \sqrt{3})$R30, [6] T=130 K, 3L C_2H_2,$(\sqrt{3} \times \sqrt{3})$R30,

[8] 77K,0.5L C_2H_2,0.25ML, [10] C_2H_2/Pt(111) at 150-300 K and C_2H_4/Pt(111) at 140-260 K,

[7] T=150 K,1.5L C_2H_2, $(\sqrt{3} \times \sqrt{3})$R30, [9] 110-120 K,

[13] 250 K, [14] pressure $< 10^{-9}$ Pa, T=92K,

[12] 80K, [11]$< 10^{-10}$ mbar,100K

S6. Adsorption energies of C_2H_2 and C_2H_4 on Pd(111)

The adsorption energies of C_2H_2 and C_2H_4 on Pd(111) are summarised in Table S6.

Table S6: The comparison of our calculated (mBEEF and RPBE) E_{ads} (in eV) with available experimental and theoretical data reported in the literature. (θ is the coverage in ML)

system	site	θ (ML)	mBEEF	RPBE	Exp.	Others.
	h-fcc	1/4	-2.31	-1.64		$\approx$-1.38[15](RPBE)
		1/4				-2.25 ,[16]-2.03 ,[17]
C_2H_2/Pd(111)		1/4				-1.91 ,[18]-1.78 [19] (PW91)
	b-par	1/4	-1.77	-1.16		-1.86,[16]-1.12[18] (PW91)
	top	1/4	changed	-0.40		-0.91,[16] -0.63[18] (PW91)
	b-par	1/4	-0.99	-0.40		$\approx$-0.38[15](RPBE)
C_2H_4/Pd(111)		1/4				-0.23[20](Tight-Binding)
		1/4				-0.86[21] (PW91)

S7. Comparison with other XC functionals and effect of van-der-Waals (vdW) corrections

To demonstrate further applications of our approach and the influence of vdW corrections, we calculated vibrational frequencies and adsorption enthalpy of C_2H_4 on the Pt(111) surface with TPSS[22], PBEsol[23], and RPBE with the Tkatchenko-Scheffler vdW correction[24] (RPBE+TS). TPSS is reported as the reliable functional for the bulk and surface properties of metals[25], and PBEsol is also widely used functional for solid systems. As shown in Figure S3a and Table S7, PBEsol gives the lowest RMSE for the vibrational frequency. TPSS shows a moderate performance among the adopted XC functionals, and there is not significant effect of the vdW correction on the accuracy of the vibrational frequency in RPBE+TS. On the other hand, as shown in Figure S3b, RPBE+TS overestimates the adsorption enthalpy compared to RPBE by 0.42 eV. Additionally, PBEsol shows the worst error among the considered functionals while the performance of TPSS is moderate.

We also investigated reaction enthalpy of the semi-hydrogenation of C_2H_2 to C_2H_4 in the gas phase. The calculated reaction enthalpy $H_r(DFA)$ is the difference of the enthalpy of each molecule in the gas phase.

$$H_r(DFA) = H_{C_2H_4} - (H_{C_2H_2} + H_{H_2})$$

$H_r(DFA)$ was compared with experimental reaction enthalpy $H_r(Exp.)$ derived from the standard enthalpy of formation.[26]

$$H_r(Exp.) = \Delta_f H^0_{C_2H_4} - \Delta_f H^0_{C_2H_2}$$

As shown in Figure S3c, RPBE showed the best performance. TPSS also showed a good performance, but mBEEF and PBEsol are not so accurate. This trend is also fit to the accuracy trend on the adsorption enthalpy.

By considering the result shown in Figure S3, RPBE is the most reliable functional for the target system because of its high accuracy for the investigated properties. On the other hand, PBEsol showed a good accuracy for the vibrational frequency, but its accuracy for the adsorption and reaction enthalpy is lower than the other functionals. These results suggest that, ideally, the assessment of the XC functionals should be based on multiple aspects. However, in practice, we are bound to use limited available measured quantities, such as vibrational frequencies, for benchmarking the calculation methods to describe metal-adsorbate systems.
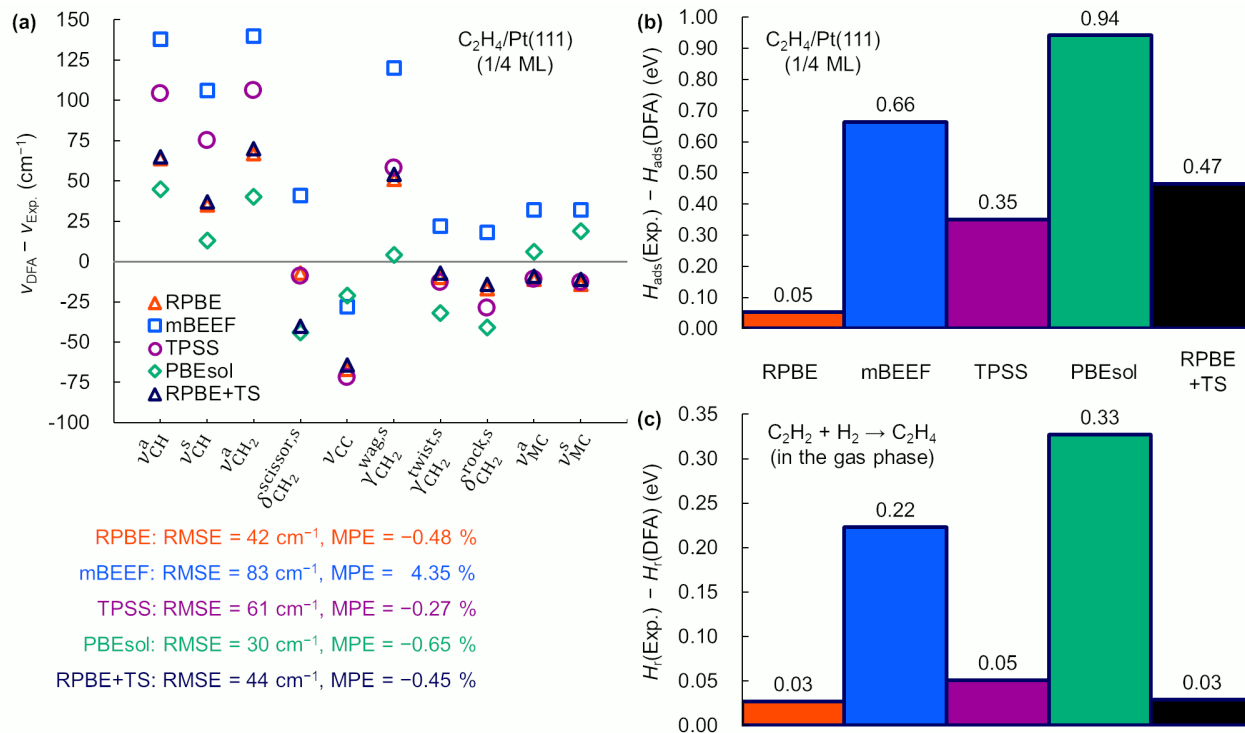
Figure S3: Investigation with other XC functionals and vdW correction. Accuracy for (a) vibrational frequencies and (b) adsorption enthalpy of the C_2H_4/Pt(111) system. Note that only vibrations of the adsorbate and its nearest-neighbor Pt atoms are considered for calculating the vibrational frequencies in these investigations. (c) Assessment for the reaction enthalpy of the semi-hydrogenation of C_2H_2 to C_2H_4 in the gas phase.

Table S7: Summary of the vibrational frequencies of the C_2H_4/Pt(111) system with other XC functionals. Note that only vibrations of the adsorbate and its nearest-neighbor Pt atoms are considered for calculating the vibrational frequencies in this investigation.

	ν^a_{CH}	ν^s_{CH}	ν^s_{CH2}	$\delta^{scissor,s}_{CH2}$	ν_{CC}	$\gamma^{wag,s}_{CH2}$	$\gamma^{twist,s}_{CH2}$	$\delta^{rock,s}_{CH2}$	ν^a_{MC}	ν^s_{MC}	RMSE (cm^{-1})	MPE (%)
Exp.[10,14]	3000	2940	2920	1430	1050	980	790	660	560	470	-	-
RPBE	3064	2975	2987	1423	983	1031	780	643	549	456	42	-0.48
mBEEF	3138	3046	3060	1471	1022	1100	812	678	592	502	83	4.35
TPSS	3104	3015	3026	1421	978	1038	777	631	549	457	61	-0.27
PBEsol	3045	2953	2960	1386	1029	984	758	619	566	489	30	-0.65
RPBE+TS	3065	2977	2990	1390	986	1034	783	646	551	459	44	-0.45

References

(1)   Harmony, M. D.; Laurie, V. W.; Kuczkowski, R. L.; Schwendeman, R.; Ramsay, D.; Lovas, F. J.; Lafferty, W. J.; Maki, A. G. Molecular structures of gas-phase polyatomic molecules determined by spectroscopic methods. *Journal of Physical and Chemical Reference Data* 1979, *8*, 619–722.

(2)   Allen Jr, H. C.; Plyler, E. K. The Structure of Ethylene from Infrared Spectra1. *Journal of the American Chemical Society* 1958, *80*, 2673–2676.

(3)   Eckerlin, P.; Hellwege, K.-H.; Kandler, H.; Hellwege, A. *Structure data of elements and intermetallic phases*; Springer, 1971; Vol. 6.

(4)   Herzberg, G. *Electronic spectra and electronic structure of polyatomic molecules*; van Nostrand, 1966; Vol. 3.

(5)   Van Lerberghe, D.; Wright, I.; Duncan, J. High-resolution infrared spectrum and rotational constants of ethylene-H4. *Journal of Molecular Spectroscopy* 1972, *42*, 251–273.

(6)   Timbrell, P.; Gellman, A.; Lambert, R.; Willis, R. Negative ion resonance selective mode enhancement in the hreel spectrum of C2H2 on Pd (111). *Surface Science* 1988, *206*, 339–347.

(7)   Gates, J.; Kesmodel, L. Thermal evolution of acetylene and ethylene on Pd (111). *Surface Science* 1983, *124*, 68–86.

(8)   Mate, C.; Kao, C.-T.; Bent, B.; Somorjai, G. The surface structure and thermal decomposition of acetylene on the Rh (111) single crystal surface and the effect of coadsorbed carbon monoxide. *Surface science* 1988, *197*, 183–207.

(9)   Bandy, B.; Chesters, M.; Pemble, M.; McDougall, G.; Sheppard, N. Low temperature electron energy loss spectra of acetylene chemisorbed on metal single-crystal surfaces; Cu(111), Ni(110) and Pd(110). *Surface Science* 1984, *139*, 87–97.

(10)   Ibach, H.; Lehwald, S. Identification of surface radicals by vibration spectroscopy: Reactions of C2H2, C2H4, and H2 on Pt (111). *Journal of Vacuum Science and Technology* 1978, *15*, 407–415.

(11)   Sock, M.; Eichler, A.; Surnev, S.; Andersen, J. N.; Klötzer, B.; Hayek, K.; Ramsey, M.; Netzer, F. High-resolution electron spectroscopy of different adsorption states of ethylene on Pd (1 1 1). *Surface science* 2003, *545*, 122–136.

(12)   Stacchiola, D.; Calaza, F.; Zheng, T.; Tysoe, W. T. Hydrocarbon conversion on palladium catalysts. *Journal of Molecular Catalysis A: Chemical* 2005, *228*, 35–45.

(13)   Chesters, M.; McCash, E. A fourier-transform reflection-absorption infrared spectroscopic study of alkyne adsorption on Cu (111). *Journal of electron spectroscopy and related phenomena* 1987, *44*, 99–108.

(14)   Steininger, H.; Ibach, H.; Lehwald, S. Surface reactions of ethylene and oxygen on Pt (111). *Surface Science* 1982, *117*, 685–698.

(15)   Studt, F.; Abild-Pedersen, F.; Bligaard, T.; Sørensen, R. Z.; Christensen, C. H.; Nørskov, J. K. Identification of non-precious metal alloy catalysts for selective hydrogenation of acetylene. *Science* 2008, *320*, 1320–1322.

(16)   Medlin, J. W.; Allendorf, M. D. Theoretical study of the adsorption of acetylene on the (111) surfaces of Pd, Pt, Ni, and Rh. *The Journal of Physical Chemistry B* 2003, *107*, 217–223.

(17) Mittendorfer, F.; Thomazeau, C.; Raybaud, P.; Toulhoat, H. Adsorption of unsaturated hydrocarbons on Pd (111) and Pt (111): A DFT study. *The Journal of Physical Chemistry B* 2003, *107*, 12287–12295.

(18) Xie, X.; Song, X.; Dong, W.; Liang, Z.; Fan, C.; Han, P. Adsorption Mechanism of Acetylene Hydrogenation. *Chinese Journal of Chemistry* 2014, *32*, 631–636.

(19) Sheth, P. A.; Neurock, M.; Smith, C. M. A first-principles analysis of acetylene hydrogenation over Pd (111). *The Journal of Physical Chemistry B* 2003, *107*, 2009–2017.

(20) Wong, Y.-T.; Hoffmann, R. A comparative study of the chemisorption of ethene on three metal surfaces: Ni (111), Pd (111) and Pt (111). *Journal of the Chemical Society, Faraday Transactions* 1990, *86*, 4083–4094.

(21) Moskaleva, L. V.; Chen, Z.-X.; Aleksandrov, H. A.; Mohammed, A. B.; Sun, Q.; Rosch, N. Ethylene conversion to ethylidyne over Pd (111): revisiting the mechanism with first-principles calculations. *The Journal of Physical Chemistry C* 2009, *113*, 2512–2520.

(22) Tao, J.; Perdew, J. P.; Staroverov, V. N.; Scuseria, G. E., Climbing the density functional ladder: nonempirical meta-generalized gradient approximation designed for molecules and solids. *Phys. Rev. Lett*. 2003, *91*, 146401.

(23) Perdew, J. P.; Ruzsinszky, A.; Csonka, G. I.; Vydrov, O. A.; Scuseria, G. E.; Constantin, L. A.; Zhou, X.; Burke, K., Restoring the density-gradient expansion for exchange in solids and surfaces. *Phys. Rev. Lett.* 2008**,** *100*, 136406.

(24) Tkatchenko, A.; Scheffler, M., Accurate molecular van der Waals interactions from ground-state electron density and free-atom reference data. *Phys. Rev. Lett.* 2009, *102*, 073005.

(25) Kabalan, L.; Kowalec, I.; Catlow, C. R. A.; Logsdail, A. J., A computational study of the properties of low- and high-index Pd, Cu and Zn surfaces. *Phys. Chem. Chem. Phys.* 2021**,** *23*, 14649-14661.

(26) Chase, M. W., Jr., NIST-JANAF Themochemical Tables, Fourth Edition. *J. Phys. Chem. Ref. Data* 1998**,** *9*, 1-1951

(27) Grube, G.; Schneider, A.; Esch, U., *Heraeus Festschrift*, 1951, *20*.

(28) Togo, A.; Chaput, L.; Tanaka, I.; Hug, G., *Phys. Rev. B*, 2010, *81*, 174301.